Zhan *et al*. *Complex Eng Syst* 2024;4:20
DOI: 10.20517/ces.2024.60

Complex Engineering Systems

Research Article

Open Access

A performance-centered design method for adaptive cruise control system

Siya Zhan[1], Congzhi Liu[2]

[1]College of Mechanical and Vehicle Engineering, Hunan University, Changsha 410082, Hunan, China.
[2]College of Mechanical and Vehicle Engineering, Chongqing University, Chongqing 400030, China.

Correspondence to: Dr. Congzhi Liu, College of Mechanical and Vehicle Engineering, Chongqing University, No. 174, Shazheng Street, Shapingba District, Chongqing 400030, China. E-mail: 15281063684@163.com; ORCID: 0000-0002-2977-1365

How to cite this article: Zhan S, Liu C. A performance-centered design method for adaptive cruise control system. *Complex Eng Syst* 2024;4:20. http://dx.doi.org/10.20517/ces.2024.60

Received: 7 Sep 2024 **First Decision:** 9 Oct 2024 **Revised:** 17 Oct 2024 **Accepted:** 1 Nov 2024 **Published:** 13 Nov 2024

Academic Editor: Hamid Reza Karimi **Copy Editor:** Fangling Lan **Production Editor:** Fangling Lan

Abstract

The adaptive cruise control (ACC) system that can take into account safety and riding comfort has attracted widespread attention. The challenges lie in designing an optimal car-following system with some predefined performance constraints based on the nonlinear dynamics, including being safe with the given certain system constraints, such as safe driving within the system input and output boundaries, also comprising the control stability. In this paper, a novel ACC design approach is proposed by transforming performance boundaries into control input and output constraints, taking into account the need for safe operation. Firstly, a nonlinear dynamics system is modeled for the ACC system based on the vehicle longitudinal dynamics. Then, a performance-centered ACC system is established based on a control barrier function and a control Lyapunov function for safety and stability concerns, respectively. Subsequently, an optimal control strategy with performance constraints is formulated and recast into a standard quadratic programming problem considering the need for stability and reliability. To validate the effectiveness of the proposed method, a real-world experiment is performed, whose results illustrate the safety performance and practical application of the ACC system.

Keywords: Adaptive cruise control, control barrier function, control Lyapunov function, quadratic programming, performance constraints.

1. INTRODUCTION

The adaptive cruise control (ACC) system has been an optional or standard equipment in commercial vehicles[1]. Its key performance is longitudinal collision avoidance and riding comfort, especially for autonomous driving vehicles[2,3]. The challenge is the potential conflicts between comfort, safety and stability, which was usually eliminated by specifying the reasonable performance function and constraint[4–6]. To guarantee driving comfort and safety, the control method with input, state or output constraints is the preferred one, such as the model predictive control (MPC)[7] and control barrier functions (CBFs)[8].

The performance balance and assurance is realized by the optimization objective and constraint condition in the MPC framework[9]. Similarly, the full state and output constraints can be actualized by the predefined CBFs or control Lyapunov functions (CLFs) of the closed-loop control system[10]. The CBF-based method also proves to be effective in the stabilization with safety problems[11], especially for the safety-critical control[12]. A safety-critical control scheme was investigated for unknown structured systems by using the CBF method[13]. An output-dependent universal barrier function was established for the consensus tracking control problem for multiagent systems with prescribed performance constraints[14]. To simultaneously consider the safety, stability, and some other performances, the CBFs and CLFs are integrated together in general, such as the quadratic programming (QP) with CBF and CLF constraints[15,16]. These attempts can balance different kinds of control performances well[17,18]. It has been shown that the optimization problem subject to the control constraints and state convergence for affine control systems can be reduced to a sequence of QPs by using CBF and CLF[15]. For example, a QP was constructed with the unification of CLF for the control objectives and CBF for the admissible state conditions, which were demonstrated on ACC and lane-keeping control problems[4,19]. Then, the optimal control input was incorporated with the performance constraints. An adaptive control scheme was developed based on the barrier Lyapunov function (BLF) for nonlinear stochastic systems with full state constraints[20]. In[21], the MPC and CBF were integrated into a complete stabilizing iteration scheme for linear discrete-time systems subject to polytopic input and state constraints. However, its calculation burden for the practical application is a huge challenge. Moreover, for the specific performance requirements of ACC systems, the safety may conflict with other performance limitations. Therefore, a performance-centered ACC strategy should be considered further for these various performances.

Effectively balancing the potential conflicts among multiple control performances, such as distance tracking, car-following stability, driving comfort, and safety of the ACC system, remains a huge challenge given system nonlinearity[22]. Furthermore, reducing computational requirements and ensuring the desired safety performance is the last important issue of its application. Thus, we explore a safe and reliable control algorithm that can guarantee safety and stability performances, which can be divided into four key parts as shown in Figure 1 and it can be constructed through four corresponding steps: dynamics modeling, CBF for the predefined safety requirement, CLF for the stability performance, and QP problem formation to solve the optimal control input. Therefore, the main contribution here is to provide a performance-centered controller considering the predefined performance requirements for the ACC systems, which lie in the following: (1) Considering the vehicle longitudinal actuator model and car-following strategy, the ACC model is characterized as a nonlinear dynamics system. For its specific model form, a CBF is designed to indirectly establish the relationship between the input and each performance constraint; and (2) An optimal control strategy with various predefined performance constraints is formulated as a standard QP problem with the CBF and CLF constraints for the safety and stability requirements, respectively. Then, a potential practical solution is obtained to enhance the control performance for ACC closed-loop systems.

The outline of this work is as follows. Section 2 establishes the ACC system model considering the input and output constraints. Section 3 describes the proposed method of the performance-centered controller. The experimental results are expressed in section 4. Finally, the main conclusions are summarized in section 5.

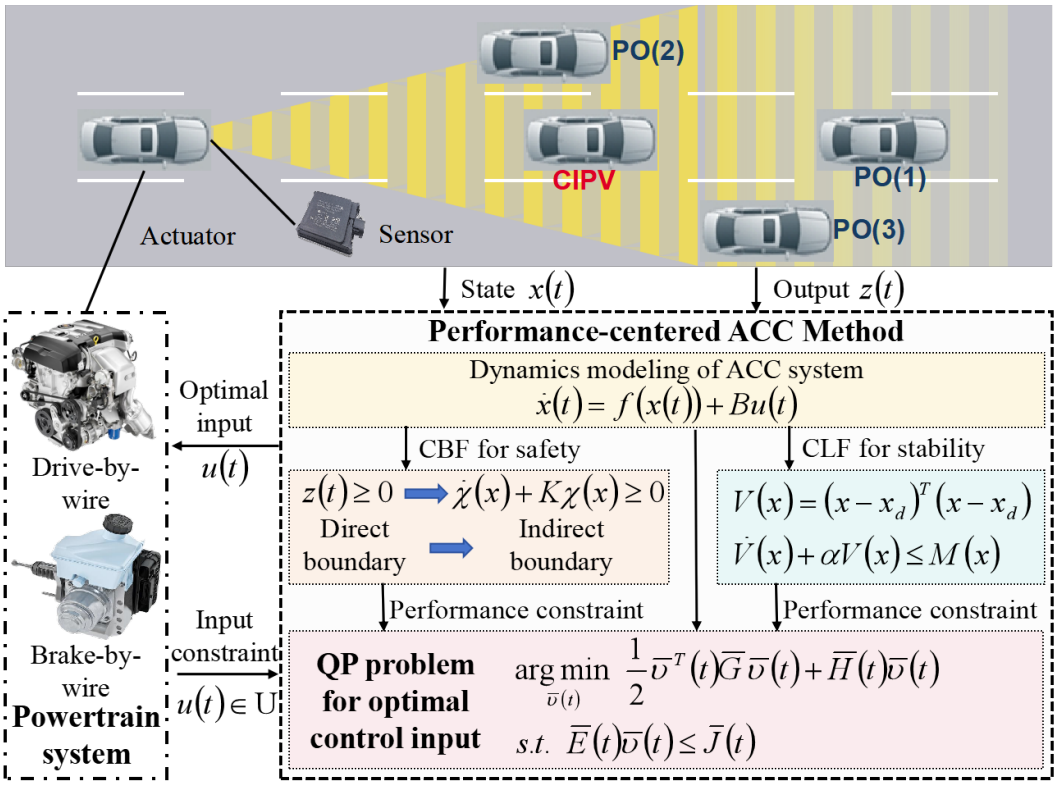

Figure 1. Frame diagram of performance-centered ACC method.

2. ACC SYSTEM MODELING

Actuator model

The actuator of the ACC system is the driving/braking-by-wire subsystem equipped on autonomous driving vehicles. The longitudinal dynamics model is to characterize the steady-state relation between the longitudinal motion and the longitudinal force of the vehicle. When the lateral and yaw motions of a vehicle are ignored, then the vehicle's longitudinal dynamics is given as

$$F_x = \delta m a_{ego} + F_{x0}, \tag{1}$$

where F_x is the total driving/braking force of a vehicle, which consists of two parts. The first one is the whole inertial force (including the rotational and translational motion resistances). The second one represents the main driving resistance which contains the rolling resistance, gradient resistance and wind drag[23], which can be given as

$$F_{x0} = \mu m g \text{sgn}(V_{ego}) \cos\theta + mg \sin\theta + \frac{C_D A}{1.632} V_{ego}^2, \tag{2}$$

where m, C_D, A are the constant weight, drag coefficient, and front face area, respectively. $\delta > 1$ is the scale factor of rotating mass to characterize the inertia of the rotating components of the chassis. $g = 9.81$ m/s^2 is the universal gravitational constant. θ is the longitudinal slope along with the driving direction of a vehicle. μ is the driving friction coefficient. V_{ego}, a_{ego} are the vehicle speed and acceleration, respectively. sgn$(\cdot)$ represents the sign function that is formed for the zero rolling resistance when the vehicle is at a standstill (i.e., $V_{ego} = 0$).

Consider the dynamics of the powertrain system as a first-order process

$$\dot{F}_x(t) = -\frac{1}{\tau} F_x(t) + \frac{1}{\tau} u(t), \tag{3}$$

where u is the external input of a driving/braking-by-wire subsystem which can be interpreted as desired driving/braking force, and τ is the time constant of a drive or brake process. Hence, the vehicle longitudinal dynamics can be characterized by the following system for the actuators:

$$\begin{aligned} &\dot{F}_x(t) = -\tfrac{1}{\tau}F_x(t) + \tfrac{1}{\tau}u(t), \\ &a_{ego} = \tfrac{1}{\delta m}F_x - \tfrac{C_D A}{1.632\delta m}V_{ego}^2 - \tfrac{1}{\delta}(\mu g \operatorname{sgn}(V_{ego})\cos\theta + g\sin\theta). \end{aligned} \tag{4}$$

Assume that the road slope and friction coefficient are slow-varying, and according to (4), the induced dynamics of acceleration can be described as:

$$\dot{a}_{ego} = -\left(\frac{1}{\tau} + \frac{C_D A V_{ego}}{0.816\delta m}\right)a_{ego} + \frac{1}{\delta m \tau}(-F_{x0} + u(t)). \tag{5}$$

Generally, the comfort performance is decided by the acceleration and jerk together, which can be indirectly judged by the input force as given in (5). Hence, the comfort constraint can be transformed into the input constraint. Then, the comfort constraint on the input should be considered and the set of control bounds is designated as follows:

$$u(t) \in \mathbb{U} \triangleq \left\{ u(t) \,\middle|\, \begin{array}{l} -c_d mg \le u(t) \le c_a mg, \\ a_{\min} \le a_{ego}(t) \le a_{\max}, \end{array} \right\}, \tag{6}$$

where the positive coefficients c_d, c_a represent the deceleration and acceleration toleration, respectively. $a_{\max}, a_{\min}$ are the acceptable maximal acceleration and deceleration, respectively.

To introduce the input regulation effect, we define

$$\begin{aligned} a_1(t) &= a_{\max} - a_{ego}(t), \\ a_2(t) &= a_{ego}(t) - a_{\min}, \end{aligned} \tag{7}$$

thus, $a_1 \ge 0, a_2 \ge 0$ is implied in the constraints (6), which can be transformed into the following performance constraints[19,24]:

$$\begin{aligned} &\dot{a}_1(t) + a_1(t) \ge 0, \\ &\dot{a}_2(t) + a_2(t) \ge 0. \end{aligned} \tag{8}$$

Then, the input constraint (6) is equivalent to

$$u(t) \in \mathbb{U} \triangleq \{u(t) : u_{\min}(t) \le u(t) \le u_{\max}(t)\}, \tag{9}$$

where

$$\begin{aligned} u_{\max} &= \min\{c_a mg, F_{x0} + \tau\delta m a_3\}, \\ u_{\min} &= \max\{-c_d mg, F_{x0} + \tau\delta m a_4\}, \\ a_3 &= a_{\max} - \left(1 - \tfrac{C_D A V_{ego}}{0.816\delta m} - \tfrac{1}{\tau}\right)a_{ego}, \\ a_4 &= a_{\min} - \left(1 - \tfrac{C_D A V_{ego}}{0.816\delta m} - \tfrac{1}{\tau}\right)a_{ego}. \end{aligned}$$

Car-following model

The main objective of the car-following mode of ACC systems is to follow the lead car with a desired safety distance which is usually established as the following headway spacing policy[25–27]:

$$d_{rel,d}(t) = d_0 + T_h V_{ego}(t), \tag{10}$$

where T_h is the time headway and d_0 is the standstill distance.

Define the spacing state for the car-following process as

$$\boldsymbol{x}(t) = \begin{bmatrix} e_d(t) \\ e_v(t) \\ a_{ego}(t) \end{bmatrix} = \begin{bmatrix} d_{rel}(t) - d_{rel,d}(t) \\ V_{obj}(t) - V_{ego}(t) \\ a_{ego}(t) \end{bmatrix}, \tag{11}$$

where d_{rel} is the relative distance between the lead car and ego car. V_{obj} is the speed of the tracked object. Then, we use the following three-order nonlinear system representation of the longitudinal dynamics for car-following characteristics [28,29]:

$$\dot{\boldsymbol{x}}(t) = \boldsymbol{f}(\boldsymbol{x}(t)) + Bu(t), \tag{12}$$

where $\boldsymbol{f}(\boldsymbol{x}(t)) = [f_1, f_2, f_3]^T$ exhibits the local Lipschitz continuity and

$$\begin{aligned} f_1 &= V_{obj}(t) - V_{ego}(t) - T_h a_{ego}(t), \\ f_2 &= a_{obj}(t) - a_{ego}(t), \\ f_3 &= -\left(\frac{1}{\tau} + \frac{C_D A V_{ego}}{0.816\delta m}\right) a_{ego} - \frac{1}{\delta m \tau} F_{x0}, \\ B &= [0, 0, \tfrac{1}{\delta m \tau}]^T, \end{aligned}$$

where a_{obj} is the acceleration of the tracked object.

Assume that the system state trajectory is predictable within the neighborhood of its desired state $\boldsymbol{x}_d = 0$ and $\dot{\boldsymbol{x}}_d = 0$ during a short control interval if the ego vehicle is driving. When the vehicle is at a standstill that $V_{ego} = 0, a_{ego} = 0$ and it wants to start driving, we introduce an offset into the desired state as $\boldsymbol{x}_d = [0, 0, a_{ref}]^T$, where a_{ref} is the referenced acceleration during the start process, which is motivated by the structure of matrix B and aims to avoid the undesirable case that the ego vehicle remains in its current standstill state and starts unsuccessfully.

Performance-centered design requirement

The safety constraint is the primary performance evaluation. Generally, a driver cannot easily drive on a narrow road at high speed or adjacent to an obstacle. Similarly, autonomous driving requires a speed reduction on a narrow road to improve the accuracy of the vehicle control. To drive more safely, the target speed should be determined by considering the environment information, such as the proximity of obstacles and collision probabilities. Moreover, the ego vehicle should maintain a safe car-following distance to avoid any potential collisions.

Hence, we define the controlled output as the speed and safe distance evaluations for the safety consideration:

$$\boldsymbol{z}(t) = \begin{bmatrix} d_{rel}(t) - d_{safe}(t) \\ V_{\text{lim}} - V_{ego}(t) \end{bmatrix}, \tag{13}$$

and the output limitations are considered as $\boldsymbol{z}(t) \geq 0$, where $V_{\text{lim}} = \min\{V_{safe}, V_{set}\}$ and $d_{safe}, V_{safe}, V_{set}$ are the safe distance, safe speed and target speed provided by the driver or autonomous driving system, respectively. Assume that $\dot{V}_{\text{lim}} = 0$ within a short time interval and $d_{safe} = 0.5d_0 + T_{safe}V_{ego}(t)$ with the safe headway as T_{safe} to prevent any potential collisions. Then, the safety performance constraint for the output is expressed as

$$\boldsymbol{z}(t) \in \mathbb{Z} \triangleq \{\boldsymbol{z}(t) \geq 0\}. \tag{14}$$

Remark 1 *If the vehicle is driving on a curved road, its safe speed satisfies the following dynamics constraint[30]:*

$$\begin{aligned} a_y &= |\kappa| V_{ego}^2 \le a_{y,\max}, \\ \omega &= |\kappa| V_{ego} \le \omega_{\max}, \end{aligned} \tag{15}$$

where κ and ω are the curvature of the road and the vehicle yaw rate which can be provided by the autonomous driving system and the chassis, respectively. $a_{y,\max}, \omega_{\max}$ are the maximal lateral acceleration and yaw rate to guarantee vehicle stability and safety during a curved road. Hence, a safe speed can be obtained as

$$V_{safe} = \min\left\{\sqrt{\frac{a_{y,\max}}{|\kappa|}}, \frac{\omega_{\max}}{|\kappa|}\right\}. \tag{16}$$

Then, vehicle safety during a curved road is also guaranteed based on the performance constraint (14).

Definition 1 *The set $\mathbb{Z}$ defined by (14) is considered forward invariant for the system (12) if all system output trajectories originating from an initial output $\boldsymbol{z}(0) \in \mathbb{Z}$ remain confined within the set $\mathbb{Z}$ for any $t \ge 0$[31].*

Lemma 1 *If there exits a continuously differentiable CBF $\boldsymbol{\chi}(\boldsymbol{x}) : \mathbb{Z} \to \mathbb{R}$, then the set $\mathbb{Z}$ is forward invariant for the system (12)[19].*

Hence, the ACC system aims to employ an input $u(t) \in \mathbb{U}$ with the output limitation $\boldsymbol{z}(t) \in \mathbb{Z}$ while ensuring that the tracking error satisfies $\|\boldsymbol{x} - \boldsymbol{x}_d\| \le \varepsilon$, where ε is a positive constant. A time-varying CBF is formulated to depict an invariant set for the controlled output of ACC systems (12):

$$\boldsymbol{\chi}(\boldsymbol{x}) = \exp\left\{\frac{\boldsymbol{z}(t)}{\|\boldsymbol{x}\| + r} - \Delta\right\} - 1, \tag{17}$$

where $r > 0, \Delta > 0$ are constants. Then, the performance constraint (14) can be guaranteed by $\chi(\boldsymbol{x}) \ge 0$. Similarly to the input constraint (8), there exists a positive constant K such that the following inequality holds for $\forall \boldsymbol{x}$ [19,24]:

$$\dot{\boldsymbol{\chi}}(\boldsymbol{x}) + K\boldsymbol{\chi}(\boldsymbol{x}) \ge 0. \tag{18}$$

Remark 2 *It is difficult to establish the direct mapping relationship between the input constraint and safety boundaries (defined as $\boldsymbol{z}(t) \ge 0$). Then, it motivates us to find an indirect way to recast the safety requirement $\boldsymbol{z}(t) \ge 0$ into an alternative form as the CBF $\boldsymbol{\chi}(\boldsymbol{x}(0)) \ge 0$, where safety is implicated in its definition (17). According to the performance constraint of the CBF (18), we can have*

$$\boldsymbol{\chi}(\boldsymbol{x}(t)) \ge \boldsymbol{\chi}(\boldsymbol{x}(0)) \exp(-Kt).$$

If the vehicle is safe at the initial sampling, i.e., $\boldsymbol{\chi}(\boldsymbol{x}(0)) \ge 0$, then it means $\boldsymbol{\chi}(\boldsymbol{x}(t)) \ge 0$ for any $t > 0$. However, an activation condition is usually adopted in the ACC system so that the initial safe state of the vehicle can be guaranteed. Hence, a predefined assumption is given here. Then, its safety performance can be maintained based on the CBF condition (18).

Assumption 1 *The initial state of the vehicle is safe when the ACC system is just activated, that is, $\boldsymbol{\chi}(\boldsymbol{x}(0)) \ge 0$.*

Then, the set (14) is forward invariant for (12) based on the definition 1, Lemma 1 and Assumption 1. According to the norm definition $\|\boldsymbol{x}\| = \sqrt{e_d^2(t) + e_v^2(t) + a_{ego}^2(t)}$, we have

$$\dot{\boldsymbol{\chi}}(\boldsymbol{x}) = (\boldsymbol{\chi}(\boldsymbol{x}) + 1) \odot \frac{\dot{\boldsymbol{z}}(\|\boldsymbol{x}\|^2 + r\|\boldsymbol{x}\|) - \boldsymbol{z}\boldsymbol{x}^T(\boldsymbol{f} + Bu)}{(\|\boldsymbol{x}\| + r)^2\|\boldsymbol{x}\|}, \tag{19}$$

where $\odot$ represents the Hadamard product and

$$\dot{\boldsymbol{z}} = C\boldsymbol{x}, C = \begin{bmatrix} 0 & 1 & -T_{safe} \\ 0 & 0 & -1 \end{bmatrix}.$$

According to (18) and (19), it yields

$$(\boldsymbol{\chi}(\boldsymbol{x})+1)\odot\frac{\boldsymbol{z}\boldsymbol{x}^{T}B}{(\|\boldsymbol{x}\|+r)^{2}\|\boldsymbol{x}\|}u(t)\leq(\boldsymbol{\chi}(\boldsymbol{x})+1)\odot\frac{C\boldsymbol{x}(\|\boldsymbol{x}\|^{2}+r\|\boldsymbol{x}\|)-\boldsymbol{z}\boldsymbol{x}^{T}\boldsymbol{f}}{(\|\boldsymbol{x}\|+r)^{2}\|\boldsymbol{x}\|}+K\boldsymbol{\chi}(\boldsymbol{x}). \tag{20}$$

To avoid that the denominator of the differential function $\dot{\boldsymbol{\chi}}(\boldsymbol{x})$ equals to zero, a simplified approximation $\|\boldsymbol{x}\|\approx\|\boldsymbol{x}\|+r$ with a small enough positive number $r=0.01$. Thus, the inequality (20) can be directly recast into the following constraint according to its safety-guaranteed implication:

$$(\boldsymbol{\chi}(\boldsymbol{x})+1)\odot\frac{\boldsymbol{z}\boldsymbol{x}^{T}B}{(\|\boldsymbol{x}\|+r)^{3}}u(t)\leq(\boldsymbol{\chi}(\boldsymbol{x})+1)\odot\frac{C\boldsymbol{x}(\|\boldsymbol{x}\|^{2}+r\|\boldsymbol{x}\|)-\boldsymbol{z}\boldsymbol{x}^{T}\boldsymbol{f}}{(\|\boldsymbol{x}\|+r)^{3}}+K\boldsymbol{\chi}(\boldsymbol{x}). \tag{21}$$

3. PERFORMANCE-CENTERED CONTROLLER

Convergence analysis

Lemma 2 *A continuously differentiable function $V(\boldsymbol{x})$ can be regarded as a CLF that ensures exponential stability of the system (12) if there exist constants $a>0,b>0,c>0$ such that*[32]

$$a\|\boldsymbol{x}\|^{2}\leq V(\boldsymbol{x})\leq b\|\boldsymbol{x}\|^{2},\forall\boldsymbol{x}$$

and

$$\inf_{u\in\mathbb{U}}\left[\dot{V}(\boldsymbol{x})+cV(\boldsymbol{x})\right]\leq 0.$$

We define a CLF for the exponential stability of the ACC system (12) according to the Lemma 2

$$V(\boldsymbol{x})=(\boldsymbol{x}-\boldsymbol{x}_{d})^{T}(\boldsymbol{x}-\boldsymbol{x}_{d})\geq 0, \tag{22}$$

then, there exist positive numbers $\beta,\gamma>0$ such that the following inequality holds for $\forall\boldsymbol{x}$

$$\beta\|\boldsymbol{x}-\boldsymbol{x}_{d}\|^{2}\leq V(\boldsymbol{x})\leq\gamma\|\boldsymbol{x}-\boldsymbol{x}_{d}\|^{2}. \tag{23}$$

Thus, there exist $\alpha>0$ and sufficiently large positive number M such that[32]

$$\dot{V}(\boldsymbol{x})+\alpha V(\boldsymbol{x})\leq M(\boldsymbol{x}), \tag{24}$$

where $M(\boldsymbol{x})\geq 0$ denotes the relaxation of the decision variable. According to the Comparison Lemma[33], it yields that

$$V(\boldsymbol{x}(t))\leq\frac{M}{\alpha}+\left(V(\boldsymbol{x}(0))-\frac{M}{\alpha}\right)\exp\left(-\alpha t\right). \tag{25}$$

According to (23) and (25), it yields

$$\|\boldsymbol{x}-\boldsymbol{x}_{d}\|\leq\sqrt{\frac{1}{\alpha\beta}\left[M+(\alpha V(\boldsymbol{x}(0))-M)\exp(-\alpha t)\right]}. \tag{26}$$

Remark 3 *Define $V_{sup}=\frac{M}{\alpha}+\left(V(\boldsymbol{x}(0))-\frac{M}{\alpha}\right)\exp\left(-\alpha t\right)$, it is clear that $0\leq\min\left\{\frac{M}{\alpha},V(\boldsymbol{x}(0))\right\}\leq V_{sup}\leq\max\left\{\frac{M}{\alpha},V(\boldsymbol{x}(0))\right\}$. Define $\varepsilon=\max\left\{\sqrt{\frac{M}{\alpha\beta}},\sqrt{\frac{V(\boldsymbol{x}(0))}{\beta}}\right\}$, then, we can obtain that $\|\boldsymbol{x}-\boldsymbol{x}_{d}\|\leq\varepsilon$, implying that the system state trajectory remains within the neighborhood of the desired state. The state deviations will be gradually eliminated if there exist some state mutations or bounded disturbances induced by the random driving behaviors of the lead vehicle, i.e., the car-following stability. Hence, the CLF restriction (24) can be employed as a lenient CLF to attain the convergence of the tracking error.*

Performance-centered controller design

The objective of ACC is to design an optimal controller with the input constraint $u(t) \in \mathbb{U}$, output limitation $\boldsymbol{z}(t) \in \mathbb{Z}$ replaced by $\chi(\boldsymbol{x}) \geq 0$ and CLF restriction (24), which possesses the notable advantage of the ability to harmonize various control performances. To achieve this goal and inspired by[15], the optimal control strategy for the ACC system is defined as the energy consumption:

$$\min_{u(t),M(\boldsymbol{x})} \int_0^t [\lambda_1(u(\tau) - F_{x0}(\tau))^2 + \lambda_2 M^2(\boldsymbol{x}(\tau)) - 2(\lambda_3 e_d(\tau) + \lambda_4 e_v(\tau))u(\tau)]d\tau, \tag{27}$$

where the three cost functions represent the energy expenditure of control input and riding comfort during the deceleration and acceleration process, the punishment of the relaxation variable, and the car-following performance trend cost, respectively. $\lambda_i > 0$ are the weight coefficients. Define the optimization variable as $\boldsymbol{\upsilon}(t) = [u(t), M(\boldsymbol{x})]^T$. The optimal objective (27) can be recast to a sequence of instantaneous optimization problems within each sufficiently small sampling interval as follows:

$$\min_{\boldsymbol{\upsilon}(t)} \frac{1}{2}\boldsymbol{\upsilon}^T(t)G\boldsymbol{\upsilon}(t) + H\boldsymbol{\upsilon}(t), \tag{28}$$

where $G = diag\{\lambda_1, \lambda_2\}, H = [-\lambda_1 F_{x0}(t) - \lambda_3 e_d(t) - \lambda_4 e_v(t), 0]$. Moreover, it should satisfy the input constraint (9), performance constraint (20) and (24), which can be transformed into the linear matrix constraint as:

$$E\boldsymbol{\upsilon}(t) \leq J, \tag{29}$$

where

$$E = \begin{bmatrix} 1 & 0 \\ -1 & 0 \\ \vartheta_1 & 0 \\ 0 & -1 \\ 2(\boldsymbol{x} - \boldsymbol{x}_d)^T B & -1 \end{bmatrix}, J = \begin{bmatrix} u_{\max}(t) \\ -u_{\min}(t) \\ \vartheta_2 \\ 0 \\ \vartheta_3 \end{bmatrix},$$

$$\vartheta_1 = (\boldsymbol{\chi}(\boldsymbol{x}) + 1) \odot \frac{z\boldsymbol{x}^T B}{(\|\boldsymbol{x}\|+r)^3},$$

$$\vartheta_2 = (\boldsymbol{\chi}(\boldsymbol{x}) + 1) \odot \frac{C\boldsymbol{x}(\|\boldsymbol{x}\|^2 + r\|\boldsymbol{x}\|) - z\boldsymbol{x}^T \boldsymbol{f}}{(\|\boldsymbol{x}\|+r)^3} + K\boldsymbol{\chi}(\boldsymbol{x}),$$

$$\vartheta_3 = -2(\boldsymbol{x} - \boldsymbol{x}_d)^T \boldsymbol{f}(\boldsymbol{x}(t)) - \alpha(\boldsymbol{x} - \boldsymbol{x}_d)^T(\boldsymbol{x} - \boldsymbol{x}_d).$$

Therefore, the optimal control strategy for the ACC system at each sampling time can be solved by the following QP problem:

$$\begin{aligned} &\arg\min_{\boldsymbol{\upsilon}(t)} \ \tfrac{1}{2}\boldsymbol{\upsilon}^T(t)G\boldsymbol{\upsilon}(t) + H(t)\boldsymbol{\upsilon}(t), \\ &s.t. \ E(t)\boldsymbol{\upsilon}(t) \leq \boldsymbol{J}(t). \end{aligned} \tag{30}$$

In some unusual circumstances, the car-following stability, comfort and safety performances may conflict, leading to a null set due to various system limitations, as given by

$$\{\upsilon(t) : E\boldsymbol{\upsilon}(t) \leq \boldsymbol{J}\} = \varnothing. \tag{31}$$

To avoid the QP problem (30) becoming infeasible and to guarantee its feasibility, a new relaxation variable $\boldsymbol{N} \geq 0$ is introduced and the QP problem (30) is recast to

$$\begin{aligned} &\arg\min_{\boldsymbol{\upsilon}(t),\boldsymbol{N}(t)} \ \tfrac{1}{2}\boldsymbol{\upsilon}^T(t)G\boldsymbol{\upsilon}(t) + \tfrac{1}{2}\lambda_5\boldsymbol{N}^T(t)\boldsymbol{N}(t) + H(t)\boldsymbol{\upsilon}(t), \\ &s.t. \ E(t)\boldsymbol{\upsilon}(t) \leq \boldsymbol{J}(t) + \boldsymbol{N}(t), \end{aligned} \tag{32}$$

which can be transformed into the standard form as

$$\begin{aligned} &\arg\min_{\bar{\boldsymbol{\upsilon}}(t)} \ \tfrac{1}{2}\bar{\boldsymbol{\upsilon}}^T(t)\bar{G}\bar{\boldsymbol{\upsilon}}(t) + \bar{H}(t)\bar{\boldsymbol{\upsilon}}(t), \\ &s.t. \ \bar{E}(t)\bar{\boldsymbol{\upsilon}}(t) \leq \bar{\boldsymbol{J}}(t), \end{aligned} \tag{33}$$

Table 1. Parameters and their effects of ACC system

Parameters	Effects description	Assignment strategy
$d_0 = 4$ m	Standstill distance	Statistics of car-following distance
$T_h = 1.2$ s, $T_{safe} = 0.6$ s	Time headway	Reaction time of driver refereed to RSS model [35]
$a_{ref} = 2$ m/s^2	Referenced acceleration	Empirical value of a comfortable start process
$a_{\max} = 2.5$ m/s^2 $a_{\min} = -5$ m/s^2	Maximal acceleration and deceleration	Acceptable comfort and safety
$c_d = c_a = 0.3$	Deceleration and acceleration toleration	Acceptable comfort and safety
$\tau = 0.18$	Time constant of chassis system	Measured value
$r = 0.01$	Constant of CBF to avoid zero denominator	Small enough positive number
$\Delta = 0.1$	Constant of CBF to guarantee safety	Very small positive number after some attempts
$K = 0.5$	Constant of CBF condition to guarantee safety	Safety condition after some attempts
$\alpha = 10$	Constant of CLF to guarantee convergence	Sufficiently large to guarantee tracking performance
$\lambda_1 = 1, \lambda_2 = 10$ $\lambda_3 = \lambda_4 = 1000, \lambda_5 = 500$	Weight coefficients of optimization objective	Magnitudes and significance of cost function

where $\bar{H}(t) = [H(t), \mathbf{0}], \bar{G} = G \bigoplus \lambda_5 I_7$ and I_7 is an identity matrix with the dimension as 7×7. The optimization variable as $\bar{\boldsymbol{v}}(t) = [u(t), M(\boldsymbol{x}), \boldsymbol{N}^T(t)]^T$. The matrices are

$$\bar{E}(t) = \begin{bmatrix} E(t) & -I \\ 0 & -I \end{bmatrix}, \bar{J}(t) = \begin{bmatrix} J(t) \\ 0 \end{bmatrix}.$$

The QP problem (33) can be solved using the interior-point method by the existing solver or toolbox [34], where the real-time solving process is omitted here.

Remark 4 *The feasibility of the proposed method with various performance constraints is guaranteed based on the penalty variable $\boldsymbol{N}(t)$. Then, the safety and stability performances established by the CBF and CLF can be considered simultaneously and their potential conflict is handled successfully. Moreover, the optimal control input is incorporated with the predefined performance limitations as the established QP problem (33), which is the key to the application of this performance-centered method.*

Remark 5 *A single vehicle ACC model (12) is considered in this paper, which can be extended to the consensus tracking control problem of cooperative adaptive cruise control (CACC) by modifying the ACC model (12) to a CACC model. For some other multiagent systems similar to [6,14], it is also available by using the reconstructed dynamic model and prescribed performance constraints.*

4. EXPERIMENTAL VERIFICATION

The whole parameters and their effects are listed in Table 1. After plenty of attempts and comparative analysis, and also according to practical experiences, the ACC performance parameters and controller parameters are given as Table 1. Then, the QP problem (33) can be solved for its real-time application. According to the magnitudes of the cost function (27), we can select the weights $\lambda_1 = 1, \lambda_2 = 10$. Based on the stability analysis of the system (12) and the characteristic of $\boldsymbol{f}, B$, the weights $\lambda_3 = \lambda_4 = 1,000$ are adopted. As safety is a key constraint, the weight $\lambda_5 = 500$ is selected.

To verify the performance of the proposed method, the field tests are conducted by a modified HAVAL SUV with drive/brake/steer-by-wire systems as shown in Figure 2, and the specification of the vehicle is given in Table 2. The vehicle is equipped with sensors such as a global navigation satellite system (GNSS)/inertial navigation system (INS) with two antennas, a yaw rate gyro equipped near the vehicle centroid, a Mobileye 560 camera installed behind the windshield, a Delphi Electronically Scanning Radar (ESR) and five Rear and Side Detection System (RSDS) Radars equipped around the car. The decision and control platform is established based on a Dspace Micro Autobox II placed in the trunk. Both signals are transmitted by the CAN-bus. The Dspace Micro Autobox II acts as the real-time controller, which receives the feedback information from the

Table 2. Experimental vehicle specifications

Item	Description
Total mass	1,700 kg
Scale factor of rotating mass	1.1
Distance from center of gravity to front axle	1.2 m
Distance from center of gravity to rear axle	1.48 m
Vehicle width	1.86 m
Vehicle length	4.6 m
Drag coefficient	0.389
Front face area	2.86 m^2

sensors and vehicle, and sends the control command to the chassis system. Then, a closed-loop ACC system is established. Because the whole perception, decision, planning and control algorithms (including the proposed method) are implemented in one embedded controller with the sampling period as 10 ms, the real-time performance is implied by the following real car experiments. To make a more intuitive comparison, three test scenarios are adopted and they are implemented in the same microprocessor with the same sampling period of 10 ms, where the first two experiments are performed by the proposed method and the third one is executed by the baseline method.

Test scenario I

To demonstrate the performances of the proposed method, a typical urban test scenario is first performed under a dynamic environment to verify the controller capabilities, which can present the results for the most relevant scenarios. To achieve a convenient and reasonable verification and enhance the applicability to real-world scenarios, the experiment is performed in a real road environment. The relative distance and safe distance of the preceding vehicle are shown in Figure 3. At the beginning (near 60 s), the car ahead is fast decelerated with the deceleration -5 m/s^2. Then, the controlled vehicle is smoothly decelerated with the maximal deceleration -1.54 m/s^2 up to the minimal speed 0.61m/s, where the actual distance is bigger than the safe distance as the partial enlarged detail in Figure 3. It can be seen that the safe car following performance can be guaranteed by the CBF (17) and its constraint condition (18). It is necessary to emphasize that a specific distance of 200 m represents a scenario in which there is no object in front of the ego vehicle. On the other hand, the sudden changing distance represents the scenarios in which there are multiple cut-in or cut-out objects, which implies that there exist some disturbances in this real road environment. According to the results, the safety performance and applicability are verified by real-world scenarios.

In this scenario, the speed limitation is $V_{\text{lim}} = 23.61$ m/s. The corresponding input, acceleration and speed are shown in Figure 4. It is clear that the constraint on the input (6) is satisfied. Moreover, the safety performance constraint (14) is guaranteed based on the CBF framework according to Figure 3 and Figure 4. According to the smooth acceleration responses, excellent riding comfort will be obtained, meaning that the proposed optimal control strategy (27) is reasonable for the ACC system. Because the limited velocity V_{lim} does not ensure safety, the optimal input is obtained by solving the QP problem and then applied to the ACC system. Then, a safe and stable ACC performance is achieved by the proposed QP-based method.

The CLF and its relaxation are shown in Figure 5, which implies that the QP problem (33) can be solved in real time according to the Figure 4 and Figure 5. Moreover, convergence is obtained during every steady car-following process, although there will be some drastic fluctuations when a cut-in or cut-out object occurs. On the contrary, the CLF will be convergent after the car-following process is steady.

The controlled outputs and their CBFs are shown in Figure 6 and Figure 7. Then, the safety performance evaluations $\boldsymbol{z}(t) \geq 0$ as defined in (14) are reflected directly. As given in (13), the output limitations $z_1 \geq 0$ and $z_2 \geq 0$ represent that the relative distance is bigger than its safe distance and the vehicle speed is slower than its limited speed, respectively, which makes it clear that the proposed method can guarantee the vehicle

Figure 2. Test vehicle and scene. (A) Experimental vehicle; (B) Test field with lane markers.

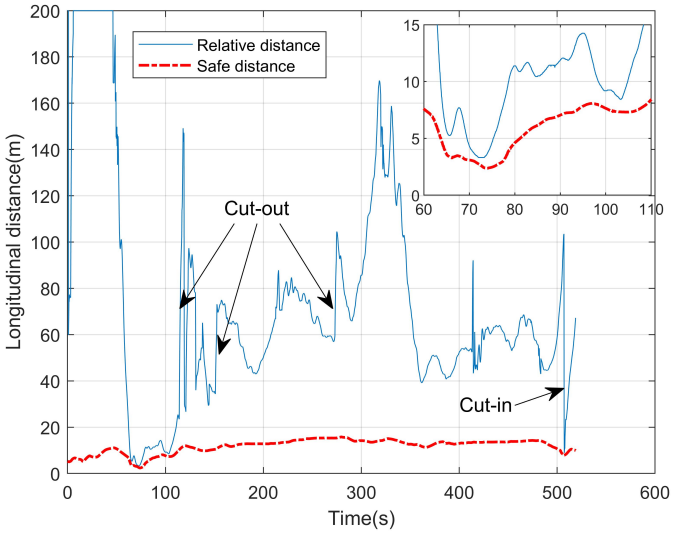

Figure 3. Actual distance and safe distance of scenario I.

collision safety and curve driving safety. The results show that the feasibility of QP problem is guaranteed by the application of CBF, CLF and slack variables, where the predefined safety and stability performances derived from the CBF and CLF are considered simultaneously. Moreover, the proposed method can balance safety, comfort and stability.

Test scenario II

The adopted second test scene is a similar but more complex urban environment with a higher traffic flow to further verify the effectiveness of the proposed method. There exist more curve driving, lane changing and cut-in or cut-out behaviors. The actual distance and safe distance of the preceding vehicle are shown in Figure 8. At the time 167s, the car ahead is fast decelerated and the controlled vehicle is decelerated with the maximal deceleration -1.57 m/s^2 up to the minimal speed of 0.43 m/s, where the minimal distance of 6.12m is also bigger than the safe distance as the partial enlarged detail in Figure 8. Then, the safety performance is guaranteed

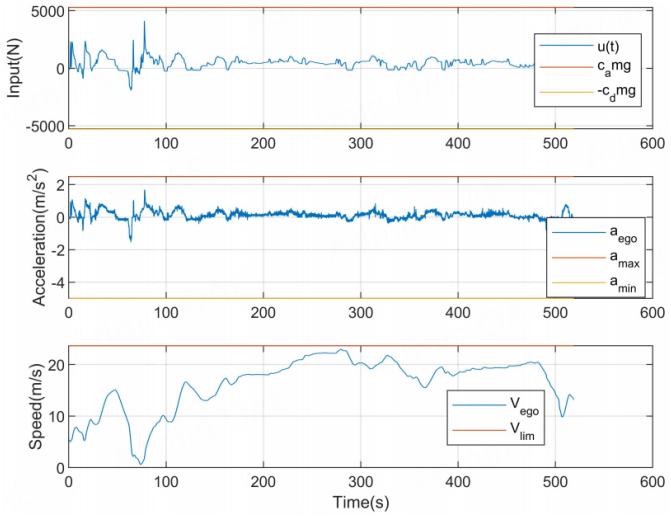

Figure 4. ACC system input and responses of scenario I.

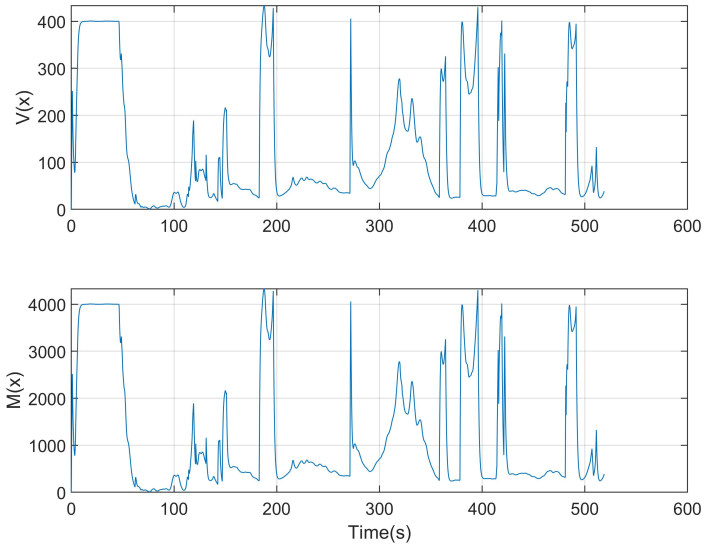

Figure 5. $V(\boldsymbol{x})$ and $M(\boldsymbol{x})$ of ACC system of scenario I.

according to the experimental results.

The input, acceleration and speed of this scenario are shown in Figure 9. It can be seen that there is a provisional parking in front of the red light and a Stop & Go driving behavior. It is obvious that the input constraint (6) is satisfied, where the comfort performance will be obtained. In addition, the vehicle can remain stationary while maintaining a safe distance during the Stop & Go condition. Moreover, the vehicle speed is much lower than its safe speed at the two obvious curve driving moments 222 and 340 s. According to the results in Figure 8 and Figure 9, the safe distance and speed are ensured during the car-following process and curve scene.

The CLF and its relaxation are shown in Figure 10, which can ensure that the QP problem (33) with the CBF and CLF constraints is solvable in real time. The controlled outputs and their CBFs are shown in Figure 11 and Figure 12. Then, the safe distance $z_1 \geq 0$ is maintained during the car-following process and the vehicle is driving with a safe speed $z_2 \geq 0$ on a curved road, which implies that vehicle safety is guaranteed by the

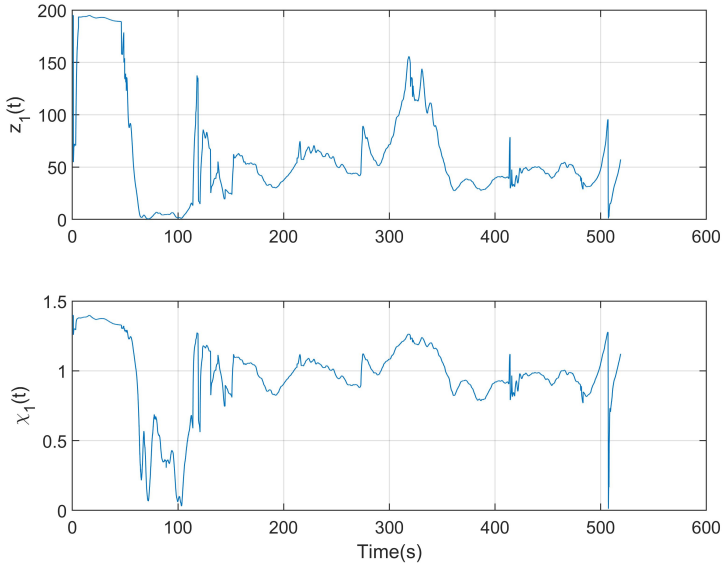

Figure 6. z_1 and its CBF of ACC system of scenario I.

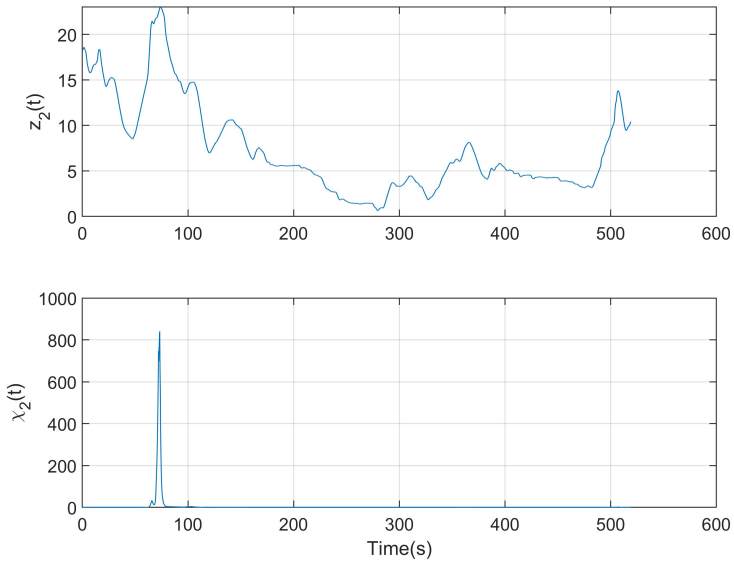

Figure 7. z_2 and its CBF of ACC system of scenario I.

proposed method.

Test scenario III

To make a further horizontal comparison, another well-known method is adopted in this test scene to validate the effectiveness of the proposed method: the intelligent driver model (IDM) method. We know that the IDM approach is a widely used method in vehicle ACC systems due to its stability and excellent calculation efficiency[36], which imitates the driving behavior habits of human drivers and will be employed as a baseline for comparison. The IDM method is a simple empirical model only with the same uncomplicated numerical

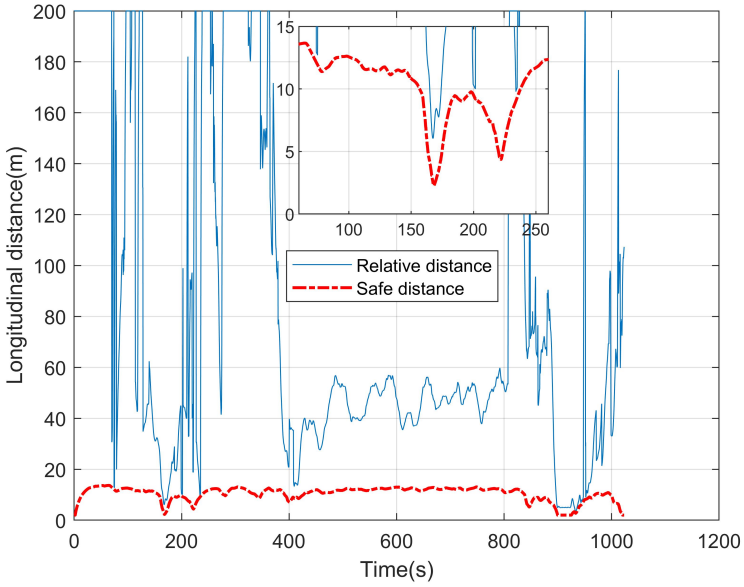

Figure 8. Actual distance and safe distance of scenario II.

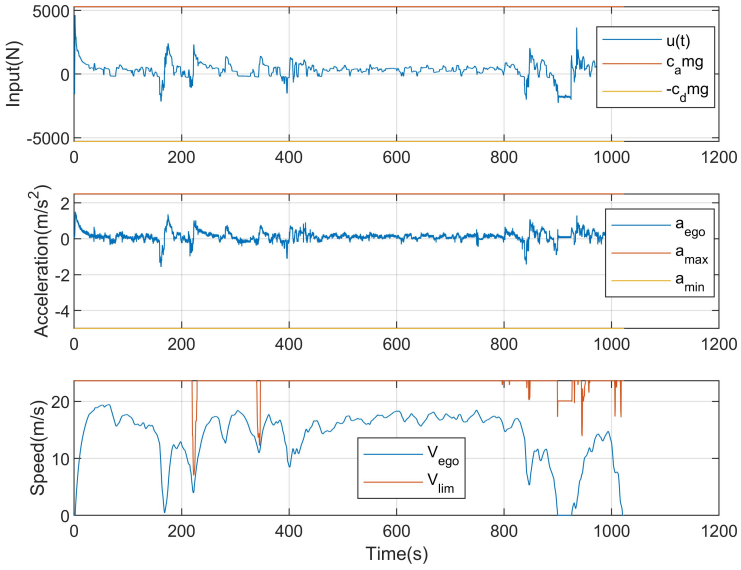

Figure 9. ACC system input and responses of scenario II.

calculation, which is defined as follows:

$$u(t) = F_{x0} + \delta c_a mg \left[1 - \left(\frac{V_{ego}}{V_{\lim}} \right)^4 - \left(\frac{d_{IDM}}{d_{rel}} \right)^2 \right], \tag{34}$$

where the desired headway is given as

$$d_{IDM} = d_0 + T_h V_{ego} + \frac{V_{ego}(V_{ego} - V_{obj})}{2g\sqrt{c_a c_d}}. \tag{35}$$

The IDM method possesses excellent computational efficiency in its practical applications as exhibited as (34). After several attempts, the proposed method and IDM can be executed with the same sampling period as 10

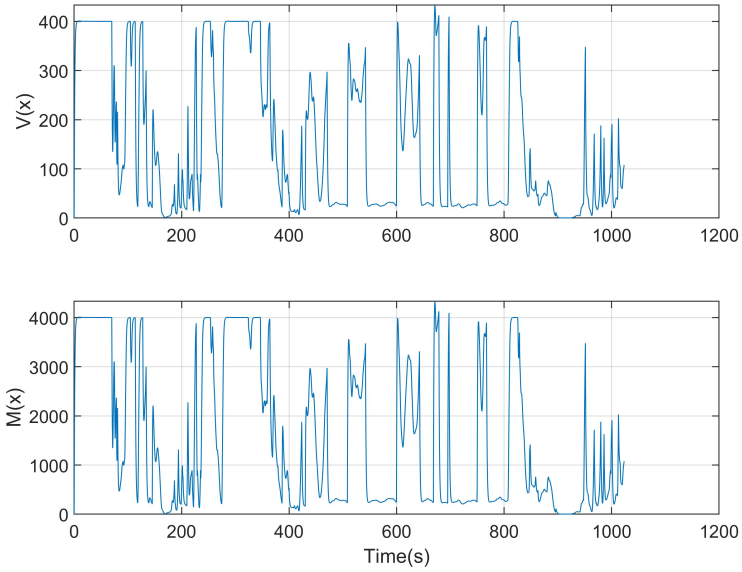

Figure 10. $V(\boldsymbol{x})$ and $M(\boldsymbol{x})$ of ACC system of scenario II.

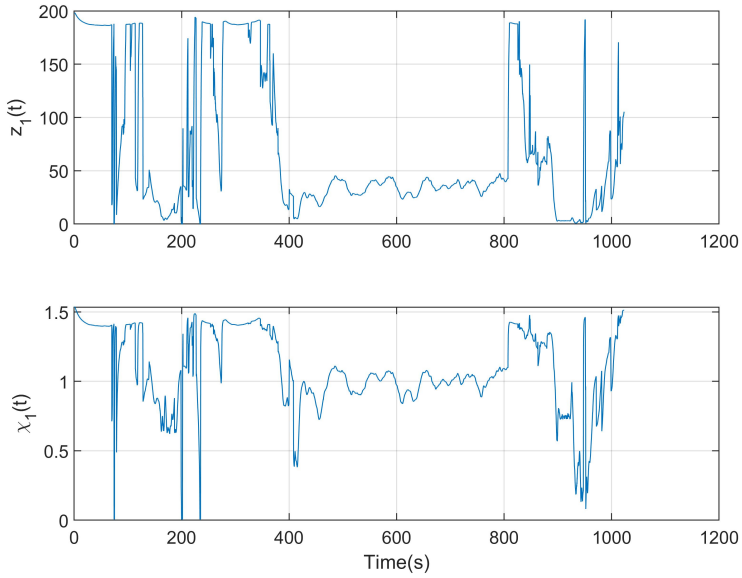

Figure 11. z_1 and its CBF of ACC system of scenario II.

ms in the real microprocessor as shown in Figure 12, which implies that the real-time calculation efficiency of the proposed method is approximate to that of the IDM method and it is satisfying for the practical application as well.

Because the experiment is carried out in real road scenarios, the surrounding vehicles are usually driven by human drivers. It is very hard to repeat the same scenarios 1 and 2 for making a reasonable comparison. Then, we adopt another similar scenario 3 on a real urban road to verify the proposed method. The relative distance and safe distance of the preceding vehicle obtained by the IDM method are shown in Figure 13, where the corresponding input, acceleration and speed are shown in Figure 14. We can see that the car-following distance is closer to its safe distance, even less than the safe distance at 216 s, where safety is hard to guarantee. The

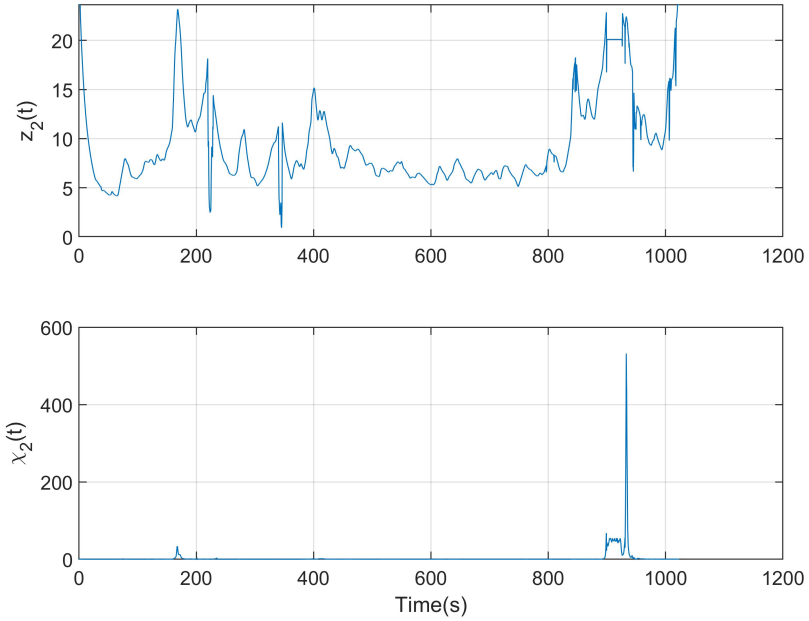

Figure 12. z_2 and its CBF of ACC system of scenario II.

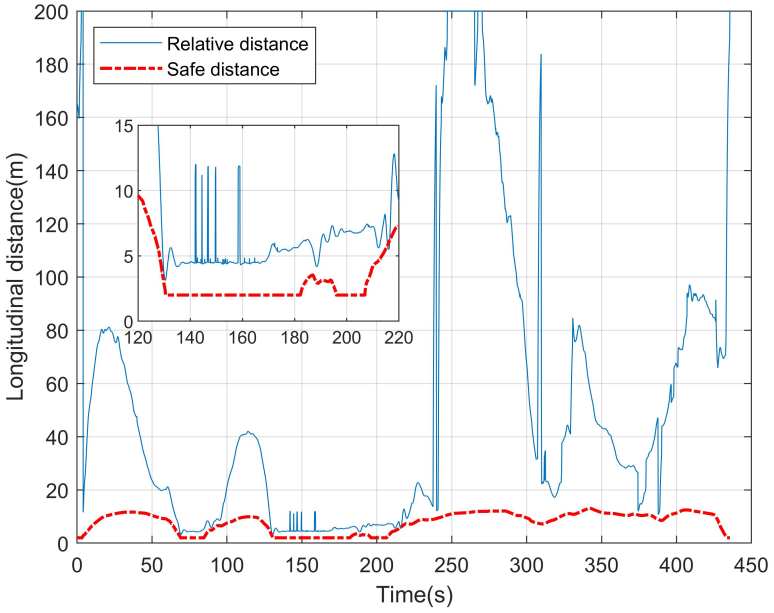

Figure 13. Actual distance and safe distance of scenario III.

maximal acceleration 1.89 m/s^2 is much bigger than that of the first two scenarios, which implies that better comfort performance can be obtained by the proposed method.

The controlled output is shown in Figure 15. It is clear that the output z_1 will be negative; i.e., the actual distance is smaller than its safe distance. Then, the safety performance requirement is not satisfied as defined in (14) since the IDM method is a controller without any constraints. On the contrary, collision safety can be guaranteed by the proposed method due to the consideration of the predefined performance constraints. Therefore, the necessity of the performance-centered design philosophy for the ACC system is verified by the

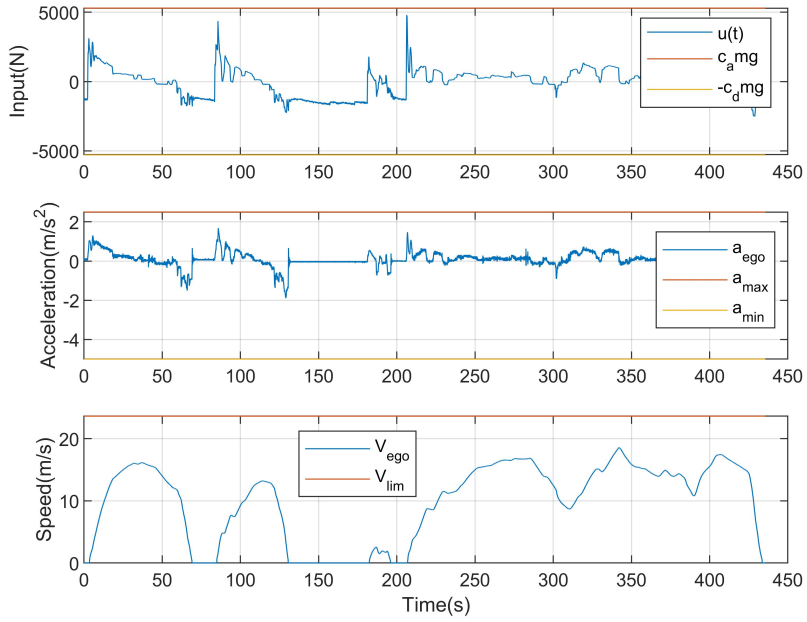

Figure 14. ACC system input and responses of scenario III.

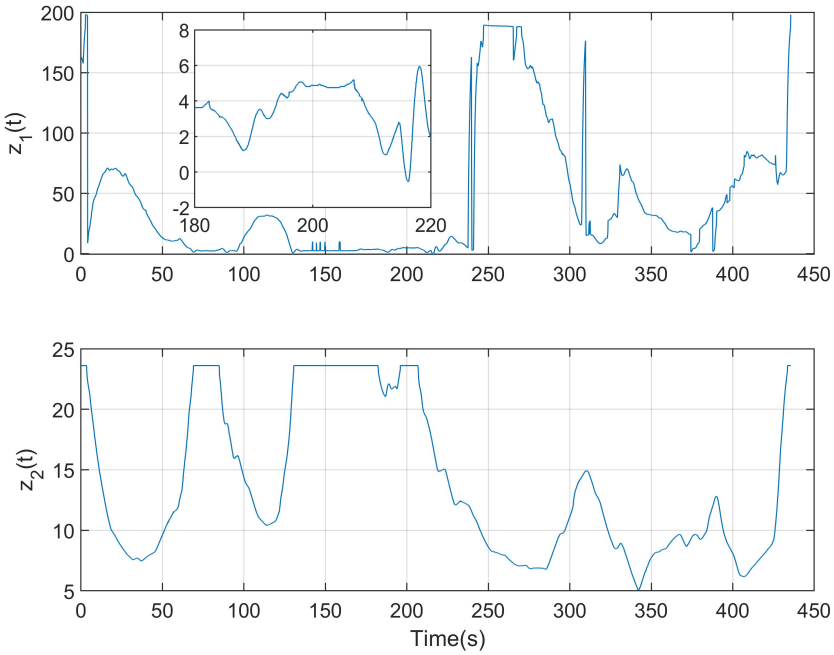

Figure 15. z_1 and z_2 of ACC system of scenario III.

comparison results. Moreover, the safety, comfort and stability performances can be overall considered.

To make a more intuitive comparison, some quantitative analysis of the performance evaluation indicators is listed in Table 3. The scenarios 1 and 2 are performed by the proposed method and the scenario 3 is performed by IDM method [36]. To further evaluate the car-following performance of the proposed controller, the root

Table 3. Experimental results comparison

Scenarios		1	2	3
Methods		Proposed method in this paper		IDM
Safety indexes	$\min(z_1)$	0.5456 m	0.12 m	-0.546 m
	$\min(z_2)$	0.6276 m/s	0.9227 m/s	5.053 m/s
Comfort indexes	$\max(\lvert a_{ego}\rvert)$	1.68 m/s^2	1.575 m/s^2	1.89 m/s^2
	RMS[1]	0.2934 m/s^2	0.3073 m/s^2	0.409 m/s^2

[1] RMS of a_{ego} for judging the comfort of the car-following performance.

mean square (RMS) value of the acceleration a_{ego} is considered, which is defined as:

$$\text{RMS} = \sqrt{\frac{1}{N}\sum_{i=1}^{N} a_{ego}^2(i)}, \tag{36}$$

where N is the sampling number of signal a_{ego}. In Table 3, the evaluation $\min(z_1) \geq 0$ and $\min(z_2) \geq 0$ are used for the safety performance. The indicators $\max(|a_{ego}|)$ and RMS are adopted for comfort and a smaller indicator implies a better comfort performance. These safety-comfort-based indicators produce a reasonable performance margin for the proposed controller. According to the results, the safety, comfort and stability performances are considered simultaneously in the proposed method. Therefore, a safer and more comfortable car-following process will be obtained by the proposed method compared with the IDM method. Moreover, the first two test scenarios are performed by the proposed method and the third one is executed by the IDM method. These experiments are implemented in the same microprocessor with the same sampling period of 10ms. Then, the real-time performance of the proposed method is verified according to the prominent computational efficiency of the IDM method.

It is worth mentioning that the proposed method is finally transformed into a QP-based optimization problem, where its essence is a kind of optimization-based approach. There are two other typical methods: linear quadratic regulator (LQR) and MPC. The LQR is an optimization method without several predefined performance constraints; then, it is hard to ensure the performance requirements. Correspondingly, the MPC is a similar optimization practice, which is usually transformed into a standard QP problem with some performance constraints. However, the MPC method is implemented by the predictive model and iterative optimization, where the calculation burden of the model predictive procedure is a huge challenge that prevents its practical application. Therefore, the proposed method can well balance the potential conflict between the multiple performance requirements, such as safety, comfort, stability and real-time performances. It can outdo the IDM, LQR and MPC methods and be used in practical applications. Then, the effectiveness of the proposed performance-centered ACC method is verified.

5. CONCLUSIONS AND DISCUSSION

In this work, the CBF and CLF are introduced and deployed on the ACC system, which provides a potential practical solution to enhance the control performance for ACC systems. Firstly, the ACC system model is modeled as a nonlinear dynamics system based on the vehicle longitudinal dynamics model and the car-following headway spacing policy. Then, the performance-centered optimal controller is established with the CBF and CLF constraints induced from various predefined performance constraints. The effectiveness of the proposed method is verified by a real road experimental scenario.

Due to the performance-centered design philosophy of the proposed method, it can also be applied in some other autonomous driving systems, such as lane-keeping or other path-tracking systems with similar nonlinear dynamics. For some other vehicle control applications, a similar approach can be adopted step-by-step: dynamics modeling, CBF established for the safety and comfort requirement, CLF established for the stability

performance, and QP problem formation to solve its control input. On the other hand, future studies will focus on the whole autonomous driving system with the safety-centered requirements for the vehicle lateral-longitudinal dynamics integrated control within more traffic scenarios such as traffic jams, also including the vehicle stability control. Moreover, the consensus tracking control and string stable problems will be considered for the CACC system or some other nonlinear multiagent systems.

DECLARATIONS

Authors' contributions

Performed data acquisition and analysis and provided administrative, technical, and material editing: Zhan S
Made substantial contributions to conception and design of the study: Liu C

Availability of data and materials

Not applicable.

Financial support and sponsorship

The authors greatly appreciate the National Science Fund of the People's Republic of China (Grant No. 52102444), the Open Foundation of the National Key Laboratory of Multi-perch Vehicle Driving Systems (Grant No. QDXT-WY-202407-16), the Zhiyuan Laboratory (Grant No. ZYL2024019) and the Central Guidance on Local Science and Technology Development Fund of Hebei Province (Grant No. 226Z2204G).

Conflicts of interest

Liu C is a Junior Editorial Board Member of the journal *Complex Engineering Systems* and the guest editor of the Special Issue of "Generalized Dynamics Modeling and Dynamics Control of Autonomous Driving Vehicle", while the other author has declared that he has no conflicts of interest.

Ethical approval and consent to participate

Not applicable.

Consent for publication

Not applicable.

REFERENCES

1. Ampountolas K. The unscented kalman filter for nonlinear parameter identification of adaptive cruise control systems. *IEEE Trans Intell Veh* 2023;8:4094-104. DOI
2. Wei P, Zeng Y, Ouyang W, Zhou J. Multi-sensor environmental perception and adaptive cruise control of intelligent vehicles using kalman filter. *IEEE Trans Intell Transport Syst* 2024;25:3098-107. DOI
3. Li Z, Zhao X, Yang J, Liu M. Model predictive control of multi-objective adaptive cruise system based on extension theory. *Complex Eng Syst* 2023;3:15. DOI
4. Xu X, Grizzle JW, Tabuada P, et al. Correctness guarantees for the composition of lane keeping and adaptive cruise control. *IEEE Trans Autom Sci Eng* 2018;15:1216-29. DOI
5. Liu C, Li L, Chen X, Yong J, Cheng S, Dong H. An innovative adaptive cruise control method based on mixed H_2/H_∞ out-of-sequence measurement observer. *IEEE Trans Intell Transport Syst* 2022;23:5602-14. DOI
6. Pan Y, Ji W, Lam H, Cao L. An improved predefined-time adaptive neural control approach for nonlinear multiagent systems. *IEEE Trans Automat Sci Eng* 2024;21:6311-20. DOI
7. Naus G, Ploeg J, Van de Molengraft M, Heemels W, Steinbuch M. Design and implementation of parameterized adaptive cruise control: an explicit model predictive control approach. *Control Eng Pract* 2010;18:882-92. DOI
8. Wang H, Peng J, Zhang F, Zhang H, Wang Y. High-order control barrier functions-based impedance control of a robotic manipulator with time-varying output constraints. *ISA Trans* 2022;129:361-9. DOI

9. Magdici S, Althoff M. Adaptive cruise control with safety guarantees for autonomous vehicles. *IFAC-PapersOnLine* 2017;50:5774-81. DOI
10. Liu YJ, Tong S. Barrier Lyapunov functions-based adaptive control for a class of nonlinear pure-feedback systems with full state constraints. *Automatica* 2016;64:70-5. DOI
11. Dong Y, Wang X, Hong Y. Safety critical control design for nonlinear system with tracking and safety objectives. *Automatica* 2024;159:111365. DOI
12. Molnar TG, Kiss AK, Ames AD, Orosz G Safety-critical control with input delay in dynamic environment. *IEEE Trans Control Syst Technol* 2023;31:1507-20. DOI
13. Wang S, Lyu B, Wen S, Shi K, Zhu S, Huang T. Robust adaptive safety-critical control for unknown systems with finite-time elementwise parameter estimation. *IEEE Trans Syst Man Cybern Syst* 2023;53:1607-17. DOI
14. Yang S, Pan Y, Cao L, Chen L. Predefined-time fault-tolerant consensus tracking control for multi-UAV systems with prescribed performance and attitude constraints. *IEEE Trans Aerosp Electron Syst* 2024;60:4058-72. DOI
15. Xiao W, Belta CA, Cassandras CG. Sufficient conditions for feasibility of optimal control problems using Control Barrier Functions. *Automatica* 2022;135:109960. DOI
16. Zhang Y, Xu M, Qin Y, Dong M, Gao L, Hashemi E. MILE: multiobjective integrated model predictive adaptive cruise control for intelligent vehicle. *IEEE Trans Ind Inform* 2023;19:8539-48. DOI
17. Gangopadhyay B, Dasgupta P, Dey S. Safe and stable RL (S^2RL) driving policies using control barrier and control Lyapunov functions. *IEEE Trans Intell Veh* 2023;8:1889-99. DOI
18. Hu C, Wang J. Trust-based and individualizable adaptive cruise control using control barrier function approach with prescribed performance. *IEEE Trans Intell Transport Syst* 2022;23:6974-84. DOI
19. Ames AD, Xu X, Grizzle JW, Tabuada P. Control barrier function based quadratic programs for safety critical systems. *IEEE Trans Autom Control* 2017; 62(8): 3861-3876. DOI
20. Liu YJ, Lu S, Tong S, Chen X, Chen CLP, Li DJ. Adaptive control-based Barrier Lyapunov Functions for a class of stochastic nonlinear systems with full state constraints. *Automatica* 2018;87:83-93. DOI
21. Feller C, Ebenbauer C. A stabilizing iteration scheme for model predictive control based on relaxed barrier functions. *Automatica* 2017;80:328-39. DOI
22. Graf Plessen M, Bernardini D, Esen H, Bemporad A. Spatial-based predictive control and geometric corridor planning for adaptive cruise control coupled with obstacle avoidance. *IEEE Trans Control Syst Technol* 2018;26:38-50. DOI
23. Sahlholm P, Johansson KH. Road grade estimation for look-ahead vehicle control using multiple measurement runs. *Control Eng Pract* 2010;18:1328-41. DOI
24. Lindemann L, Dimarogonas DV. Control barrier functions for signal temporal logic tasks. *IEEE Control Syst Lett* 2019;3:96-101. DOI
25. Rajamani R, Zhu C. Semi-autonomous adaptive cruise control systems. *IEEE Trans Veh Technol* 2002;51:1186-92. DOI
26. Naus GJL, Vugts RPA, Ploeg J, van de Molengraft MJG, Steinbuch M. String-stable CACC design and experimental validation: a frequency-domain approach. *IEEE Trans Veh Technol* 2010;59:4268-79. DOI
27. Brugnolli MM, Pereira BS, Angélico BA, Maria Laganá AA. Adaptive cruise control with a customized electronic control unit. *J Control Autom Electr Syst* 2019;30:9-15. DOI
28. Sheikholeslam S, Desoer CA. Longitudinal control of a platoon of vehicles with no communication of lead vehicle information: a system level study. *IEEE Trans Veh Technol* 1993;42:546-54. DOI
29. Stankovic SS, Stanojevic MJ, Siljak DD. Decentralized overlapping control of a platoon of vehicles. *IEEE Trans Control Syst Technol* 2000;8:816-32. DOI
30. Rajamani R. Vehicle dynamics and control. London: Springer Science; 2006.
31. Glotfelter P, Cortes J, Egerstedt M. Nonsmooth barrier functions with applications to multi-robot systems. *IEEE Control Syst Lett* 2017;1:310-5. DOI
32. Ames AD, Galloway K, Sreenath K, Grizzle JW. Rapidly exponentially stabilizing control Lyapunov functions and hybrid zero dynamics. *IEEE Trans Autom Control* 2014;59:876-91. DOI
33. Drazin PG, Drazin PD. Nonlinear systems, 3rd ed. USA: Cambridge University Press; 1992.
34. Jorge Nocedal SW. Numerical Optimization, 2nd ed. Springer series in operations research. Berlin, Germany: Springer; 2006.
35. Chai C, Zeng X, Wu X, Wang X. Evaluation and optimization of responsibility-sensitive safety models on autonomous car-following maneuvers. *Transp Res Rec J Transp Res Board* 2020;2674:662-73. DOI
36. Li Z, Li W, Xu S, Qian Y. Stability analysis of an extended intelligent driver model and its simulations under open boundary condition. *Phys A Stat Mech Appl* 2015;419:526-36. DOI